Efficient Modeling of Excitable Cells Using Hybrid Automata*

Pei Ye[1], Emilia Entcheva[2], Radu Grosu[1], and Scott A. Smolka[1]

[1] Department of Computer Science, Stony Brook University
[2] Department of Biomedical Engineering, Stony Brook University

Abstract. We present an approach based on hybrid automata (HA), which combine discrete transition graphs with continuous dynamical systems, to modeling complex biological systems. Our goal is to efficiently capture the behavior of excitable cells previously modeled by systems of nonlinear differential equations. In particular, we derive HA models from the Hodgkin-Huxley model of the giant squid axon, the Luo-Rudy dynamic model of a guinea pig ventricular cell, and a model of a neonatal rat ventricular myocyte. Our much simpler HA models are able to successfully capture the action-potential morphology of the different cells, as well as reproduce typical excitable cell characteristics, such as refractoriness (period of non-responsiveness to external stimulation) and restitution (adaptation to pacing rates). To model electrical wave propagation in a cell network, the single-cell HA models are linked to a classical 2D spatial model. The resulting simulation framework exhibits significantly improved computational efficiency in modeling complex wave patterns, such as the spiral waves underlying pathological conditions in the heart.

1 Introduction

Systems biology is an emerging multidisciplinary field, whose goal is to provide a systems-level understanding of biological systems, by uncovering the structure, dynamics and control methods of these systems [21]. While many exciting and profound advances have been made in investigating robustness, network structures and dynamics, and application to drug discovery, systems biology is still in its infancy.

An important open problem in systems biology is finding appropriate computational models that scale well for both the simulation and formal analysis of biological processes. Currently, the majority of these models are given in terms of large and complex sets of nonlinear differential equations, describing in painful detail the underlying biological phenomena. Although an invaluable asset for understanding local interactions, such models are often not amenable to formal analysis and may render simulation at the organ or even the cell level impractical. See, however, [7].

* R. Grosu and P. Ye were partially supported by the NSF Faculty Early Career Development Award CCR01-33583.

Considering this state of affairs, systems biology could greatly benefit from the development of abstraction techniques that, given a system of nonlinear differential equations, (semi-automatically) construct a more abstract model for which the properties of interest are preserved. One promising technique is Hybrid automata [16, 1], which intuitively replace short-lived, transient behaviors with discrete transitions. A hybrid automaton (HA) includes both discrete and continuous dynamical variables. The discrete variables define the automaton's modes of behavior. The continuous variables are governed by mode-dependent differential equations. Hybrid automata have been used as mathematical models for a variety of embedded systems, including automated highway systems, air traffic management, embedded automotive controllers, robotics and real-time circuits. More recently, they have been used to model the behavior of biological systems [13, 12, 11, 20, 2].

In abstracting a system of nonlinear differential equations to an HA, one can follow a *rational* approach, by analyzing the particular form of the equations; or an *empirical* approach, by analyzing the shape of the curves obtained via numerical integration. The rational approach is appealing because the resulting HAs are likely to be closely related to the original biological phenomena. However, the larger the system of equations, the harder it becomes to perform the abstraction. The empirical approach is appealing because, as shown in Sect. 3.1, it is often independent of the number of equations. Moreover, as a "curve fitting" technique first trained on a formal model, it can be subsequently applied on experimental data.

The main goal of this paper is to prove the feasibility and illustrate the benefits of the empirical abstraction technique. The particular biological processes we consider are networks of excitable cells. Brain, heart and skeletal muscle share similar properties of excitable tissue, featuring both discrete behavior (all-or-nothing response to electrical activation) and continuous behavior (recovery to rest follows a temporal path, determined by multiple competing ion flows).

The classical mathematical models of excitable cells [17, 24, 4] involve complex systems of nonlinear differential equations. Starting from each model, we manually construct a four-state HA that captures essential excitable-cell behavior (reentrance in particular), is amenable to formal analysis, and exhibits a nearly ten-fold speedup in a simulation of a 400-by-400 cell network. The states of the HA are directly derived from the biological interpretation of the action potential (AP) curve, which was derived via numerical integration.

The rest of the paper is organized as follows. Sect. 2 describes the excitable behavior of cardiac cells, while Sect. 3 reviews their classic mathematical models. Sect. 3.1 presents our corresponding HA models, while Sect. 3.2 contains our simulation results. Sect. 4 concludes with directions for future work.

2 Biological Background

Our focus in this paper is on the efficient modeling of cardiac cells, which serve as a primary example of excitable tissue. The rhythmic, pump-like function

of the heart is driven by muscle contractions, which are triggered by electrical signals. On each beat, a control electrical signal is generated by the sinoatrial node, the heart's internal pacemaking region. Electrical waves then travel along a prescribed path, exciting cells in the main chambers of the heart (atria and ventricles) and assuring synchronous contractions. At the cellular level, the electrical signal is a change in the potential across the cell membrane, and is caused by the flow of ions between the inside and outside of the cell. The major ion species involved in this process are sodium, potassium and calcium; they flow through multiple voltage-gated ion channels (pore-forming proteins in the cell membrane). Excitation disturbances can occur in the behavior of these ion channels at the cell level, or in the propagation of the electrical waves at the cell network level. Computational tools can help better understand both of these pathological conditions.

Cardiac Action Potential. The electrical signal at the cellular level for each excitation event is known as an *action potential* (AP). Action potentials for ventricular cells (the major portion of the heart muscle) are externally triggered events: a cell fires an action potential as an all-or-nothing response to a supra-threshold electrical signal, and each AP follows more or less the same sequence of events and has the same magnitude regardless of the applied stimulus. After an initial step-like increase in the membrane potential, an AP lasts for a couple of hundred milliseconds in most mammals. During the AP, no re-excitation can occur, which is a safety mechanism to ensure the reliable working of the heart. The early portion of an AP is known as the "absolute refractory period" due to its non-responsiveness to further stimulation. The later portion of an AP is known as the "relative refractory period", during which an altered secondary excitation event is possible if the stimulation threshold is raised.

There are considerable differences in AP duration, morphology and underlying ion currents for different species and different regions in the heart. Nevertheless, all APs exhibit the following major phases (see Fig. 1): resting, rapid upstroke, early repolarization, plateau or later repolarization, and final repolarization (identical to the resting phase due to the cyclic nature of an AP).

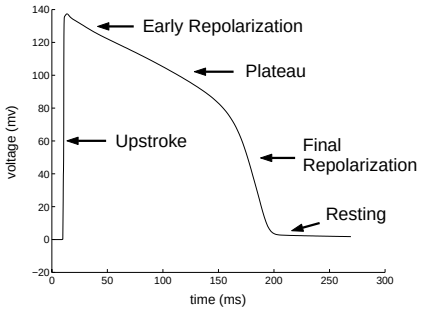

Fig. 1. Major AP phases.

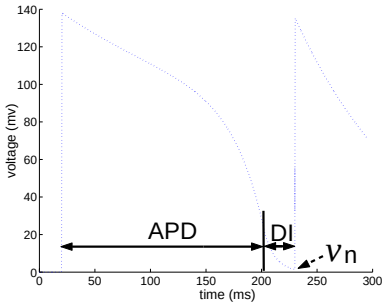

Fig. 2. APD and DI time periods.

The resting phase features a constant transmembrane potential (difference between the inside and outside potential of the cell) of about -80mV for most

species; i.e. the membrane is polarized at rest. During the AP upstroke, the transmembrane potential rapidly changes (over the course of a couple of milliseconds) from negative to positive; i.e. the membrane *depolarizes*. This is followed by an early repolarization phase, between the upstroke and the following plateau. A slower, plateau phase is present in most mammalian action potentials, during which calcium influx facilitates the muscle contraction. A faster final repolarization brings the potential back to the resting phase. Because of their universal nature among species and regions, the AP phases served as a natural guide in the construction of our hybrid-automaton models.

When a cardiac cell is subjected to repeated stimuli, two important time periods can be identified: the *action potential duration* (APD), the time the cell is in an excited state, and the *diastolic interval*, the time between the "end" of the action potential and the next stimulus. Figure 2 illustrates the two intervals. The function relating APD to DI is called the APD *restitution function*. The relationship is nonlinear and captures the phenomenon that the longer the recovery time, the closer in duration a subsequent APD is to the current one.

3 Mathematical Models of Excitation

Mathematical modeling of ionic processes that underly cell excitation dates back to 1952, when Hodgkin and Huxley formulated their model of a squid giant axon [17]. This laid the framework for subsequent models of increasing complexity, using multiple continuous state variables (voltage, ion channel gates, ion concentrations) to describe the action potentials in different cell types [24, 4, 19, 8, 23]. Current models of cardiac cells include more than 20 such state variables and a very large number of fitted parameters.

At the opposite end of the spectrum, oversimplified discrete models emerged, based on cellular automata [10, 6]. These models do not attempt to truthfully represent the morphology or intricacies of the action potentials, but rather view the excitation process as a finite state machine with simple rules of state transitions. This approach has been criticized for its ad hoc rules and failure to capture essential features, such as response to pacing. Our HA models fall between the classical differential equation approach and the discrete cellular automata approach, attempting, as much as possible, to retain the authenticity of the former and the efficiency of the latter.

The Hodgkin-Huxley Model (HH). The first quantitative description of cellular excitation was empirically developed by Hodgkin and Huxley (HH) for a squid giant axon [17]. The HH model includes three ionic currents: fast inward sodium, outward potassium, and a time-independent linear (leak) current. The generalized form of the HH model is as follows,

$$C\dot{V} = -\overline{g}_{\mathrm{Na}} m^3 h (V - E_{\mathrm{Na}}) - \overline{g}_{\mathrm{K}} n^4 (V - E_{\mathrm{K}}) - \overline{g}_{\mathrm{L}} (V - E_{\mathrm{L}}) + I_{\mathrm{st}}$$
$$\dot{y} = (y - y_\infty)/\tau_y, \quad y_\infty = \varphi_y(V), \quad \tau_y = \psi_y(V), \quad y \leftarrow m, h, n$$

where: V is transmembrane voltage [mV], whose changes form the AP; $\overline{g}_{\mathrm{Na}}$,$\overline{g}_{\mathrm{K}}$,$\overline{g}_{\mathrm{L}}$ are the maximum channel conductance [mS/μF] for the sodium, potassium and

the leakage channel, respectively; E_{Na},E_{K},E_{L} are reversal potentials [mV] for the sodium, potassium and the leakage channel, respectively; m, h, n are the ion channel gates, following the differential equations obtained by substituting m,h and n for y, where y_∞ and τ_y are voltage-dependent functions, representing the steady-state and the time-constant of a gate; C is the cell capacitance [μF] and I_{st} is the stimulation current [$\mu\mathrm{A}/\mu\mathrm{F}$].

Luo-Rudy Guinea Pig Ventricular Cell Model (LRd). In a series of papers, Y. Rudy et al. developed some of the most detailed cardiac cell models to date, targeting a guinea pig AP [24, 23, 18]. The ion channel description in these models is similar to the one given in HH, but a much larger number of ion currents is included. The complexity of this class of models is further increased by the addition of active ion pumps, intracellular compartments for calcium transport, and calcium buffers. A detailed description of the LRd model is omitted here.

Neonatal Rat Ventricular Cell Model (NNR). Among the mammalian species, the mouse and the rat have a substantially different AP morphology—much more triangular with almost absent plateau phase—compared to the AP simulated by the LRd model. Neonatal rats are often used as an experimental model in cardiac electrophysiology, and a computational model is a desirable tool. A neonatal rat model (NNR), derived from the LRd model, is being developed by Entcheva et al. (unpublished). Our HA model for NNR has the same structure as our HA LRd model, with adjusted parameters to replicate the behavior of this detailed ionic model.

3.1 Modeling Cardiac Excitation using Hybrid Automata

A *hybrid automaton* (HA) H is an extended finite automaton, consisting of the following components [16]:

- A finite set $X = \{x_1, \ldots, x_n\}$ of real-numbered *variables*. The number n is called the *dimension* of H. We write $\dot{X}$ for the set $X = \{\dot{x}_1, \ldots, \dot{x}_n\}$ of dotted variables (which represent first derivatives during continuous change), and X' for the set $X = \{x'_1, \ldots, x'_n\}$ of primed variables (which represent values at the conclusion of discrete steps).
- A finite, discrete *control graph* (V, E). The vertices in V are called *control modes*. The edges in E are called *control switches*.
- Vertex-labeling functions *init*, *inv* and *flow* assigned to each control mode $v \in V$. Initial condition $\mathit{init}(v)$ and invariant condition $\mathit{inv}(v)$ are predicates whose free variables are from X. Flow condition $\mathit{flow}(v)$ is a predicate whose free variables are from $X \cup \dot{X}$.
- Edge-labeling function *jump* assigned to each control switch $e \in E$. Jump condition $\mathit{jump}(e)$ is a predicate whose free variables are from $X \cup X'$. Associated with each jump is zero or more *actions*, which reset the value of variables in X.
- A finite set Σ of *events*, and an edge-labeling function *event* that assigns to each control switch an event.

An HA has a natural graphical representation as a state transition diagram, with control modes as the states and control switches as the transitions. Flows and invariants (predicates within curly braces) appear within control modes, while jump conditions (in square brackets) and actions appear near the control switches. Continuous variables are in lower case (v,v_x, etc); constant parameters in the flows are in Greek (α_x^0, etc); constants in invariants and jump conditions are in upper case (V_{T}, etc), the same as events (V_{S}). All the constant values are given in Table 1 in the end of this section.

General HA template for excitable cells. Piecewise linear HA models are attractive because they offer rich descriptive power, while still amenable to formal analysis. The basic idea of our method is to find such HAs (non-linearity may occur as stated later), containing as few continuous variables as possible, and accurately depicting cell excitation behavior. The empirical method we use is basically a curve-fitting technique, where the curve being fitted has the linear form $\dot{V} = AV$. The dimension of V for the HH, LRd and NNR model is 2,3 and 3, respectively. Experimental analysis showes that at least two variables are needed for a faithful simulation. While the variables in V are not directly connected to the ones in the ODE model, they essentially represent the degrees of freedom in the ODE model.

All of our HA models associate a control mode with each major AP phase: *resting and final repolarization (FR)*, *stimulated*, *upstroke*, and *plateau and early repolarization (ER)*. Initially, the cell is in *resting and FR*. When (externally) stimulated with the event V_{S}, it enters mode *stimulated* and updates its voltage according to the stimulus current. Upon termination of the stimulation, via event $\overline{V}_{\mathrm{S}}$, with a sub-threshold voltage, the cell returns to *resting* without firing an AP. If the stimulus is supra-threshold, i.e., $v \geq V_{\mathrm{T}}$ holds, the excited cell will generate an AP by progressing to mode *upstroke*. The recovery course of the cell follows transitions to mode *plateau and ER* and then to *resting and FR*. The jump conditions on the control switches monitor the transmembrane potential v, rather than imposing a rigid timing scheme. This approach allows for AP adaptation (response to various pacing frequencies).

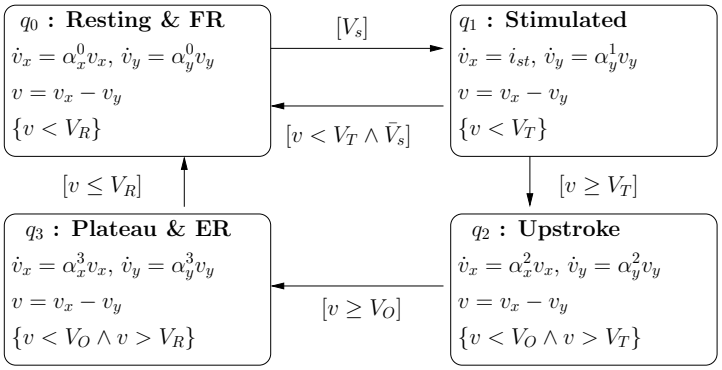

Fig. 3. Hybrid automaton for HH model.

HA for the HH model. The HA model for HH is given in Fig. 3. Variables v_{x} and v_{y} define a second-order system of linear differential equations in each control mode, while i_{st} is the excitation current and V_S is the stimulation event. The membrane voltage $v = v_{\mathrm{x}} - v_{\mathrm{y}}$ is used to control mode switches. The initial mode is q_0. The mode invariants are given below the differential equations describing the membrane voltage. Like the jump conditions, they depend on three (albeit different) model-specific constants (see Table 1): *threshold voltage* V_{T}, *overshoot voltage* V_{O}, and *repolarization voltage* V_{R}.

HA for the LRd model. Our HA model for LRd can be seen as an extension of the one for HH. In particular, to properly represent the longer-maintained plateau phase of the cardiac AP and to capture its frequency adaptation, additional variables v_{z} and v_{n} are introduced. The need for v_{z} in the LRd and NNR models can be explained by the complexity increase in the ion fluxes between neurons and cardiac cells; namely, calcium flux plays a profound role in the maintenance of the AP plateau for proper cardiac-muscle contraction to occur.

Restitution-related variable v_{n} (read v "next", see Fig 2) is used to modify the overall voltage by recording the voltage at the termination of the DI; i.e., upon the arrival of a new stimulation. It is known that the immediate memory of an excitable cell is directly linked to the DI: a shorter DI results in a shorter following AP, while a longer DI produces a longer AP [5]. This simple memory model helps capture the proper response of AP to pacing frequency, which is an essential feature of the cardiac excitation. Accordingly, we define $\theta = v_{\mathrm{n}}/V_{\mathrm{R}}$ and incorporate the function $f(\theta) = 1 + 13\sqrt[6]{\theta}$ (our choice of a 6th root function is inspired by the fact that the APD is not proportional to DI but a convex function of it—see Fig. 8) into mode *Plateau and ER*, which mainly determines the length of the APD. The resulting HA (Fig 4) is, however, no longer linear. It is an interesting question whether this nonlinearity can be removed.

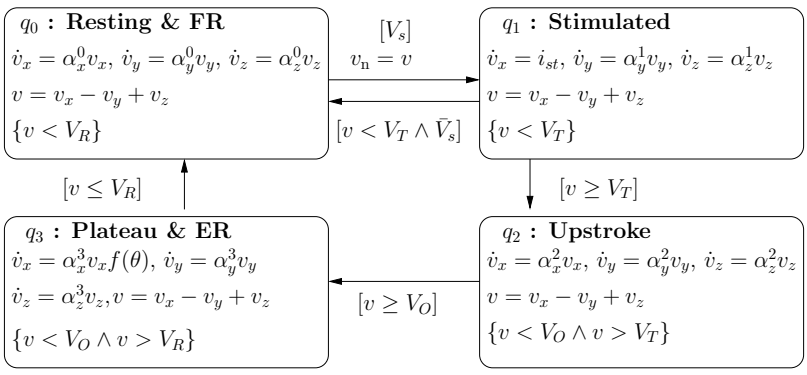

Fig. 4. Hybrid automaton for LRd model.

HA for the NNR Model. Our HA model for NNR is defined in Fig. 5, where $f(\theta) = 1+2\theta$. For better modeling of cell-to-cell interactions in cardiac excitation, the threshold and overshoot do not remain constant during simulation. Instead, they also become a function of θ, and are defined as follows: $g(V_{\mathrm{T}}) = V_{\mathrm{T}} \cdot (1 + 1.45\sqrt[6]{\theta})$ and $h(V_{\mathrm{O}}) = V_{\mathrm{O}} - 40 \cdot \sqrt{\theta}$.

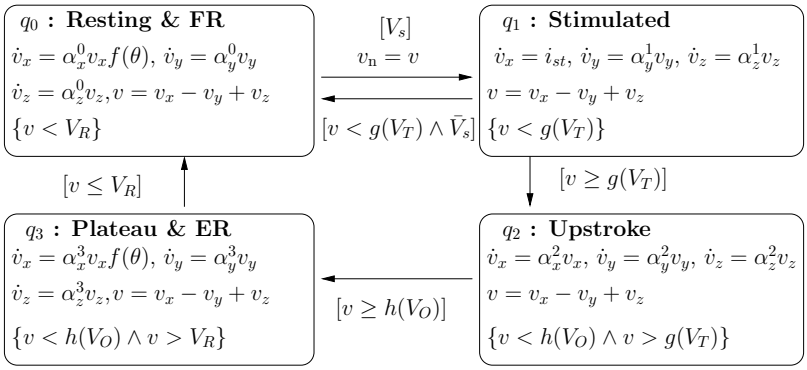

Fig. 5. Hybrid automaton for NNR model.

Parameter definitions. The values of the coefficients and constants occurring in the HH, LRd and NNR HA models are summarized in Table 1. They were obtained either from the cited literature or empirically through experimentation.

	HH	**LRd**	**NNR**		**HH**	**LRd**	**NNR**
V_{R}	10	20	20	α_{z}^1	N/A	-0.1	-0.2
V_{T}	10	20	30	α_{x}^2	1.4	200	250
V_{O}	83	138	120	α_{y}^2	15	0	200
α_{x}^0	-0.98	-0.1	-0.025	α_{z}^2	N/A	100	125
α_{y}^0	-0.16	-0.1	-0.07	α_{x}^3	-0.98	-0.001	-0.025
α_{z}^0	N/A	-0.1	-0.2	α_{y}^3	-0.16	0.036	-0.07
α_{x}^1	N/A	N/A	N/A	α_{z}^3	N/A	0.008	-0.2
α_{y}^1	-0.16	-0.1	-0.07				

Tbl. 1: Parameter definitions.

cell array size	**original**	**hybrid**
2×2 cell array	5 s	3 s
4×4 cell array	9 s	3 s
8×8 cell array	26 s	6 s
16×16 cell array	93 s	14 s
32×32 cell array	365 s	51 s
64×64 cell array	1460 s	198 s
400×400 cell array	61833 s	8018 s

Tbl. 2: Computational efficiency.

3.2 Simulation Results

We present simulation results obtained with our HA models of excitable cells. The results demonstrate that our simulations are both accurate and efficient. For the HH and LRd models, the membrane potential (v) is offset such that the resting potential is 0 mv. The time unit in all three models is milliseconds and the voltage is in millivolts except Table 2 which shows the computation time in seconds of the simulation for both HA and NNR model. The voltage of each time step is integrated using Euler method.

HH model. For the HH model, simulations were conducted at the single-cell level. For the case of a solitary action potential firing successfully, results are given in Fig. 6 for both the original HH model and our derived HA model.

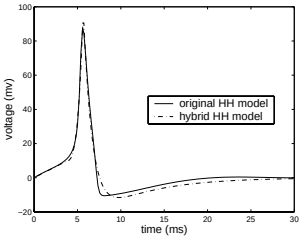

Fig. 6. AP in HH model.

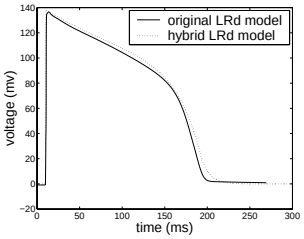

Fig. 7. AP in LRd model.

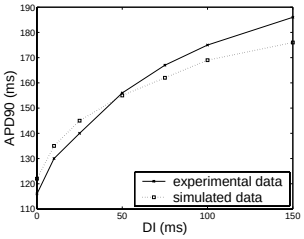

Fig. 8. Simulated LRd RC.

LRd model. Figure 7 compares the AP for the HA model with that of the original model. The simulated electrical restitution curve (response to pacing frequencies) for the LRd model is given in Fig. 8. The plot relates the preceding diastolic interval (DI) and the subsequent action potential duration at 90% recovery (APD90). It can be seen that, in contrast to cellular automata models, our hybrid model captures the *frequency sensitivity* of the original ODE model. Thus, we have achieved sensitivity to frequency without maintaining explicit timers, but rather by relying strictly on voltage-related parameters.

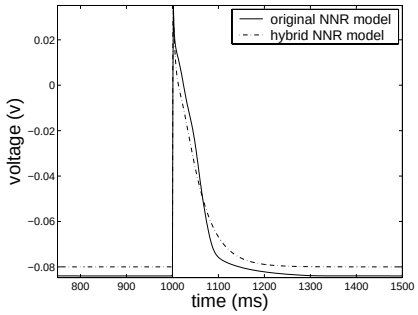

Fig. 9. AP in NNR model.

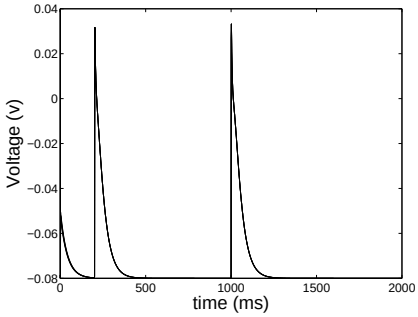

Fig. 10. AP for 2×2 HA array.

NNR model. To simulate the cardiac cell excitation propagation in homogeneous tissues, we need, in addition to a single-cell model, a diffusion model that describes the relationship of a cell with its neighbors. Here, we use a classic spatial 2D model as our diffusion model. The comparison of a single cell's solitary AP is demonstrated in Fig. 9. Figure 10 shows our results on a 2×2 cell array when three outside stimuli are delivered. The first stimulus does not cause an action potential, while the following two trigger a full response. For small grids, the high cell-to-cell coupling causes all cells to respond simultaneously.

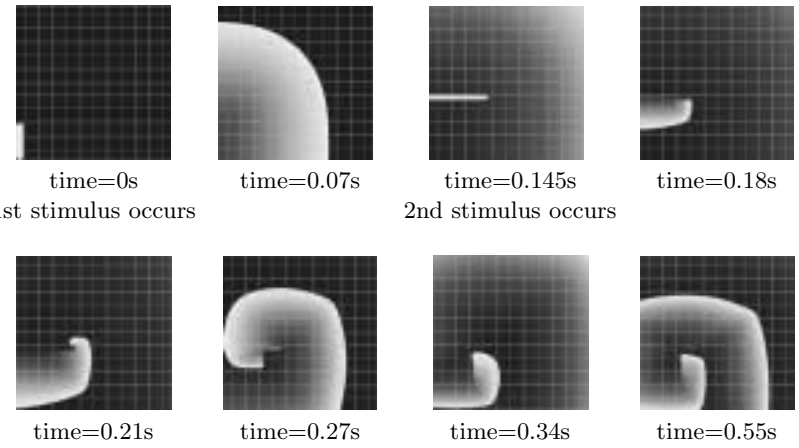

Fig. 11. Snapshots during spatial simulation of excitation propagation in Hybrid model.

We extended the simulations to model cell arrays as large as 400×400 cells. In these spatial simulations, the stimulation conditions (location and timing of the stimuli) were varied to simulate classical phenomena typical for cardiac tissue [25, 14, 15]. Running the original NNR model and the derived HA model under the same stimulation protocols, we observed similar spatiotemporal patterns (including spiral waves, in Fig. 11). This suggests that the proposed reduced hybrid automaton not only captures the AP morphology for a single cell, but also correctly models the system in multicellular conditions when cell-to-cell communication in propagating the AP is critical. Thus, we show for the first time that the hybrid automaton modeling approach is a suitable framework for modeling multicellular excitable tissue. Additionally, a substantial improvement in computational efficiency was observed with the hybrid model, as shown in Table 2. The benefit of the computational simplicity and scalability of the developed hybrid model will become especially valuable for large-scale 2D and 3D simulations with millions of cells.

4 Conclusions and Related Work

Representing the complex response of excitable cells with piecewise-linear approximate HA models permits fully analytical solutions in the different phases of the excitation cycle, therefore providing a framework for analytical analysis regardless of the complexity of the system. This is particularly important when one is concerned with issues of stability and rhythm disturbance upon stimulation in both neurons and cardiac cells. Additionally, the piecewise linearization of the system and the reduced representation increase efficiency of computation without abstracting away essential system features.

A previous study [9] derived a piecewise linear affine representation of the HH model and analyzed the behavior of the system as a function of the stimulus

intensity. In that simplified 2-parameter, 9-state hybrid model, the phase plane behavior of excitation events was correctly reproduced for a subset of tested cases, but the AP morphology was oversimplified and did not match the original model. We present in this study an alternative linearization approach and derive a hybrid automaton that offers a superior representation of the AP and has the flexibility to match a variety of AP shapes and responses (from neuronal to cardiac). Other related work includes [26], where another linearization technique, based on Taylor expansion, is successfully applied to biochemical pathways; [22], who argue in favor of hybrid automata as an efficient framework for reasoning about complex biological processes; and [3], who propose the application of bisimulation and collapsing techniques on HA models of biological systems for the qualitative analysis of their temporal evolution.

We are currently experimenting with the use of optimization techniques to derive HA model parameters. This should further improve both the efficiency and precision of our HA models, while allowing us to further simplify model complexity. Future work includes the analytical analysis of stability based on the derived hybrid automaton, and the mathematical exploration of arrhythmia-prone (unstable) modes. To better understand the spatiotemporal behavior of electrical waves in cardiac tissue, we plan to improve and simplify the diffusion modeling. In particular, the implementation of specialized neighborhood operators is expected to provide further computational gain over the currently employed classical diffusion model.

Acknowledgments: We would like to thank the anonymous referees for their valuable comments.

References

1. R. Alur, C. Courcoubetis, T. A. Henzinger, and P. Ho. Hybrid automata: An algorithmic approach to the specification and verification of hybrid systems. In *Proceedings of Hybrid Systems*, pages 209–229, 1992.
2. K. Amonlirdviman, R. Ghosh, J. D. Axelrod, and C. J. Tomlin. A hybrid systems approach to modeling and analyzing planar cell polarity. In *Proceedings of the International Conference on Systems Biology*, Stockholm, December 2002.
3. M. Antoniotti, C. Piazza, A. Policriti, M. Simeoni, and B. Mishra. Taming the complexity of biochemical models through bisimulation and collapsing: theory and practice. *Theor. Comput. Sci.*, 325(1):45–67, 2004.
4. G. W. Beeler and H. Reuter. Reconstruction of the action potential of ventricular myocardial fibres. *J Physiol*, 268:177–210, 1977.
5. R. D. Berger. Electrical restitution hysteresis - good memory or delayed response? *Circulation Research*, 94:567–569, 2004.
6. G. Bub, L. Glass, N. Publicover, and A. Shrier. Bursting calcium rotors in cultured cardiac myocyte monolayers. In *Proc Nat Acad Sci USA*, volume 95, pages 10283–10287, 1998.
7. E. J. Crampin, N. P. Smith, and P. J. Hunter. Multi-scale modelling and the IUPS physiome project. *J. Mol. His.*, 35(7):707–714, 2004.

8. D. DiFrancesco and D. Noble. A model of cardiac electrical activity incorporating ionic pumps and concentration changes. *Philos Trans R Soc Lond B Biol Sci*, 307:353–398, 1985.
9. J. G. Dumas and A. Rondepierre. Modeling the electrical activity of a neuron by a continuous and piecewise affine hybrid system. In *Hybrid Systems: Computation and Control*, pages 156–171, 2003.
10. M. Gerhardt, H. Schuster, and J. J. Tyson. A cellular automation model of excitable media including curvature and dispersion. *Science*, 247:1563–1566, 1990.
11. R. Ghosh, A. Tiwari, and C.J. Tomlin. Automated symbolic reachability analysis, with application to delta-notch signaling automata. Lecture Notes in Computer Science. Springer-Verlag, 2003.
12. R. Ghosh and C. J. Tomlin. Hybrid system models of biological cell network signaling and differentiation. In *Proceedings of the 39th Annual Allerton Conference on Communications, Control, and Computing*, Monticello, IL, October 2001.
13. R. Ghosh and C. J. Tomlin. Lateral inhibition through delta-notch signaling: A piecewise affine hybrid model. volume 2034 of *Lecture Notes in Computer Science*, Rome, Italy, March 2001. Springer-Verlag.
14. R. A. Gray and J. Jalife. Spiral waves and the heart. *Int J Bifurc Chaos*, 6:415–435, 1996.
15. R. A. Gray, A. M. Pertsov, and J. Jalife. Spatial and temporal organization during cardiac fibrillation. *Nature*, 392:75–78, 1998.
16. T. A. Henzinger. The theory of hybrid automata. In *Proceedings of the 11th IEEE Symposium on Logic in Computer Science*, pages 278–293, 1996.
17. A. L. Hodgkin and A. F. Huxley. A quantitative description of membrane currents and its application to conduction and excitation in nerve. *J Physiol*, 117:500–544, 1952.
18. T. J. Hund, N. F. Otani, and Y. Rudy. Dynamics of action potential head-tail interaction during reentry in cardiac tissue: ionic mechanisms. *Am J Physiol Heart Circ Physiol*, 279:1869–79, 2000.
19. P. Hunter, P. McNaughton, and D. Noble. Analytical models of propagation in excitable cells. *Progr Biophys Mol Biol*, 30:99–144, 1975.
20. I. Hwang, H. Balakrishnan, R. Ghosh, and C.J. Tomlin. Reachability analysis of delta-notch lateral inhibition using predicate abstraction. In *Proceedings of High Performance Computing*, Bangalore, December 2002.
21. H. Kitano. Computational systems biology. *Nature*, 420:206–210, 2002.
22. P. Lincoln and A. Tiwari. Symbolic systems biology: Hybrid modeling and analysis of biological networks. In R. Alur and G. Pappas, editors, *Hybrid Systems: Computation and Control HSCC*, volume 2993 of *LNCS*, pages 660–672. Springer, March 2004.
23. C.-H Luo and Y. Rudy. A model of the ventricular cardiac action potential - depolarisation, repolarisation and their interaction. *Circulation Research*, 68, 1991.
24. C. H. Luo and Y. Rudy. A dymanic model of the cardiac ventricular action potential: I. simulations of ionic currents and concentration changes. *Circ Res*, 74:1071–1096, 1994.
25. G. Moe, W. Rheinboldt, and J. Abildskov. A computer model of atrial fibrillation. *Am Heart J*, 67:200–220, 1964.
26. M. A. Savageau. *Biochemical Systems Theory*. Addison-Wesley, 1976.